REGULAR ARTICLE

blood advances

Reduced bone formation in males and increased bone resorption in females drive bone loss in hemophilia A mice

M. Neale Weitzmann,[1,2,*] Susanne Roser-Page,[1] Tatyana Vikulina,[2] Daiana Weiss,[2] Li Hao,[2] W. Hunter Baldwin,[3] Kanglun Yu,[4] Natalia del Mazo Arbona,[4] Meghan E. McGee-Lawrence,[4,5] Shannon L. Meeks,[3] and Christine L. Kempton[6,*]

[1]Atlanta VA Medical Center, Decatur, GA; [2]Division of Endocrinology and Metabolism and Lipids, Department of Medicine, Emory University School of Medicine, Atlanta, GA; [3]Aflac Cancer and Blood Disorders Center of Children's Healthcare of Atlanta, Department of Pediatrics, Emory University, Atlanta, GA; [4]Department of Cellular Biology and Anatomy and [5]Department of Orthopaedic Surgery, Medical College of Georgia, Augusta University, Augusta, GA; and [6]Department of Hematology and Medical Oncology, Emory University School of Medicine, Atlanta, GA

Key Points

- Male and female *F8*^{TKO} hemophilia A mice failed to attain peak BMD, an event that predisposes humans to early bone fracture later in life.
- Reduced bone volume in *F8*^{TKO} mice results from suppressed bone formation in male mice but increased bone resorption in female mice.

Hemophilia A (HA), a rare X-linked recessive genetic disorder caused by insufficient blood clotting factor VIII, leaves affected individuals susceptible to spontaneous and traumatic hemorrhage. Although males generally exhibit severe symptoms, due to variable X inactivation, females can also be severely impacted. Osteoporosis is a disease of the skeleton predisposing patients to fragility fracture, a cause of significant morbidity and mortality and a common comorbidity in HA. Because the causes of osteoporosis in HA are unclear and in humans confounded by other traditional risk factors for bone loss, in this study, we phenotyped the skeletons of *F8* total knockout (*F8*^{TKO}) mice, an animal model of severe HA. We found that trabecular bone accretion in the axial and appendicular skeletons of male *F8*^{TKO} mice lagged significantly between 2 and 6 months of age, with more modest cortical bone decline. By contrast, in female mice, diminished bone accretion was mostly limited to the cortical compartment. Interestingly, bone loss was associated with a decline in bone formation in male mice but increased bone resorption in female mice, a possible result of sex steroid insufficiency. In conclusion, our studies reveal a sexual dimorphism in the mechanism driving bone loss in male and female *F8*^{TKO} mice, preventing attainment of peak bone mass and strength. If validated in humans, therapies aimed at promoting bone formation in males but suppressing bone resorption in females may be indicated to facilitate attainment of peak mass in children with HA to reduce the risk for fracture later in life.

Introduction

Hemophilia A (HA) is a disease characterized by the decrease or absence of functional factor VIII (FVIII), a protein necessary for blood clotting.[1] Because HA is X linked, the disease predominates in males.[2] Females may carry a single copy of the HA gene and are usually asymptomatic carriers or mildly symptomatic but in rare cases may also express severe phenotypes with joint hemorrhage and other disease- and treatment-related complications.[3]

With proper diagnosis and modern treatment options, including clotting factor replacement, products free of pathogenic viruses such as HIV and hepatitis C virus, and improved medical management provided by specialized hemophilia treatment centers (particularly in the United States), mortality rates for hemophilia patients have declined substantially.[4] However, the gains in patient health now being reaped through improved health care are offset in part by comorbidities, including osteoporosis, a disease of the skeleton that predisposes patients to bone fracture.[5]

Submitted 19 October 2018; accepted 7 January 2019. DOI 10.1182/bloodadvances.2018027557.

*M.N.W. and C.L.K. contributed equally to this study as lead investigators.

The full-text version of this article contains a data supplement.

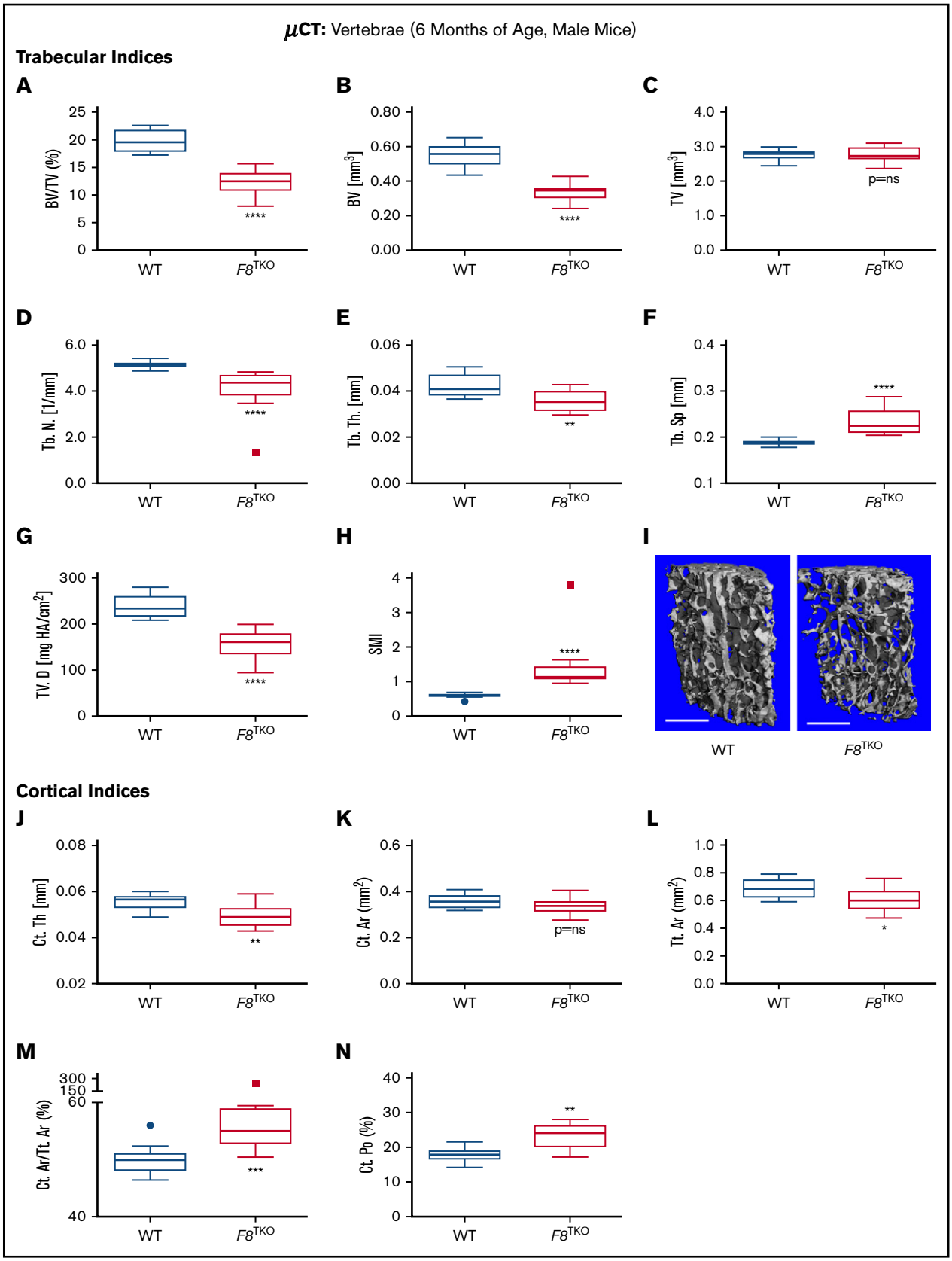

Figure 1. μCT analysis of lumbar vertebrae in skeletally mature WT and *F8*^{TKO} male mice. Six-month-old male C57BL6 WT and *F8*^{TKO} mice L3 vertebrae were analyzed by high-resolution (6 μm) μCT and independent trabecular and cortical bone compartments segregated. (A-H) Trabecular indices (A) BV/TV, (B) BV, (C) TV, (D) Tb.N,

Indeed, osteopenia (low bone mineral density [BMD]) and osteoporosis are highly prevalent in HA. In a recent study by our group, 38% of adult men ≥50 years of age with HA were found to have osteoporosis.[6] In a study of young adults (median age, 41.5 years) Gerstner et al found that 70% of HA patients exhibited decreased BMD, with 43% displaying osteopenia and 27% osteoporosis.[7]

Low bone mass in HA leads to fracture rates that are significantly elevated in HA patients.[8] Hip fractures cause 1-year mortality rates as high as 32%,[9] while vertebral fractures can cause chronic disabling pain and deformity.[10] Patients frequently experience a significant decline in quality of life, and psychological issues such as depression and anxiety are common.[10]

The causes of low bone mass in HA are likely multifactorial, and risk factors for low BMD are often present in HA populations, including low vitamin D levels, low body mass index, lower activity scores, and HIV and hepatitis C virus infections.[7] HIV infection is a significant risk factor for low BMD, and HIV-1 antiretroviral therapy further exacerbates bone loss by promoting inflammatory events associated with immune regeneration.[11-13] Bone loss in HA patients has been found to be enhanced significantly by HIV infection and is associated with the severity of arthropathy.[6,14] However, in the study by our group, only 42% of the variation in bone mass was explainable by clinical variables such as HIV, severity of arthropathy, alcohol intake, race, and body mass index.[6]

Mechanistically, whether bone loss is related to changes in bone formation or bone resorption, or both, is controversial. In a study of children with HA, low osteocalcin, a serum marker of bone formation, predominated in the group with low BMD, while no differences in bone resorption were observed.[15] In contrast, in children with severe HA, another study found an increase in bone resorption and significantly diminished bone formation,[16] as did a study of children on anticoagulant therapy, which was found to be an independent predictor of bone resorption and bone formation markers.[17] In addition, a study of young boys with HA reported that both indices of resorption and formation were elevated.[18] A study of adults with hemophilia found that multiple markers of bone resorption were significantly increased, while 1 of 2 markers of bone formation was also diminished.[14]

These conflicting data are difficult to reconcile. Invasive mechanistic studies in human populations are notoriously difficult to perform, and HA in the human context is complex, as there are numerous risk factors for low BMD that may be present in different individuals. To augment clinical studies, animal models of HA have been developed. A preliminary bone phenotyping study of a factor VIII (FVIII)–deficient animal model of HA identified a bone phenotype characterized by diminished femoral BMD and cortical thickness in male mice.[19] In a follow-up study, diminished bone mass was consistent with increased bone resorption, but no significant changes in bone formation were identified.[20]

In this present study, we used a new animal model of severe F8 hemophilia, with a complete *F8* total knockout ($F8^{TKO}$),[1] to study the etiology and kinetics of HA bone accretion and decline in mice. Our data revealed that impaired bone formation in young male $F8^{TKO}$ mice and increased bone resorption in female mice led to a failure to attain peak BMD and that sexual dimorphic effects on bone turnover and loss may need to be considered in the treatment of HA patients.

Materials and methods

All reagents were purchased from Millipore Sigma (St. Louis, MO) unless otherwise indicated.

Mice

Studies were approved by the Animal Care and Use Committee of Emory University and conducted in accordance with the National Institutes of Health Laboratory Guide for the Care and Use of Laboratory Animals.

HA mice are total FVIII gene knockout mice ($F8^{TKO}$) and have been backcrossed into a >95% C57BL/6 background as judged by single-nucleotide polymorphism analysis.[1] Wild-type (WT) littermates from the breeding colony were used as controls.

Mice were housed under specific-pathogen-free conditions. The animal facility was kept at 23°C (±1°C) with 50% relative humidity and a 12:12-hour light/dark cycle.

Bone densitometry

Dual-energy X-ray absorptiometry (DXA) was performed to quantify BMD (g/cm^2) in isolated femurs, tibias, and lumbar spines ex vivo using a PIXImus 2 bone densitometer (GE Medical Systems) as previously described.[21]

Quantitative bone histomorphometry

Bones were calcein labeled 10 and 3 days before euthanization. Dynamic histomorphometric indices, including mineral apposition rate (MAR) and bone formation rate (BFR/bone surface [BS]), were measured in the cancellous bone of 5 μm undecalcified and unstained calcein-labeled sections. VonKossa/MacNeals Tetrachrome–stained slides were used to quantify osteoblast number and osteoblast surface and osteoclast number and osteoclast surface quantified on tartrate-resistant acid phosphatase stained sections counterstained with fast green. All slides were digitized using a microscope (Olympus IX-70) and digital camera (QIcam) and analyzed at original magnification ×200 or ×400 using image analysis software (Bioquant Osteo, Nashville TN).

Microcomputed tomography

Microcomputed tomography (μCT) was performed as previous described[11,21] using a μCT40 scanner (Scanco Medical AG, Brüttisellen, Switzerland) with a voxel size of 6 μm (70 kVp and 114 mA, with a 200-ms integration time). We analyzed 400 tomographic slices at the L3 vertebra (2.4 mm) and 300 slices at the distal femoral metaphysis (1.8 mm). Trabecular bone was segmented from the cortical shell for a total area of 1.8 mm beginning ~0.5 mm from the distal growth plate.

Figure 1. (continued) (E) Tb.Th, (F) Tb.Sp, (G) volumetric density (TV.D), and (H) SMI. (I) Representative high-resolution (6-μm) 3D visual reconstructions of L3 vertebrae. Scale bars represent 500 μm. (J-N) Cortical indices (J) Ct.Th, (K) Ct.Ar, (L) Tt.Ar, (M) Ct.Ar fraction (Ct.Ar/Tt.Ar), and (N) cortical porosity (Ct.Po). All data are expressed as boxplots (median + IQR) with Tukey whiskers. n = 10 WT and 11 $F8^{TKO}$ mice/group. *$P < .05$, **$P < .01$, ***$P < .001$, ****$P < .0001$, and ns (not significant) by Student *t* test or Mann-Whitney *U* test (Tb.N and Ct.Ar/Tt.Ar).

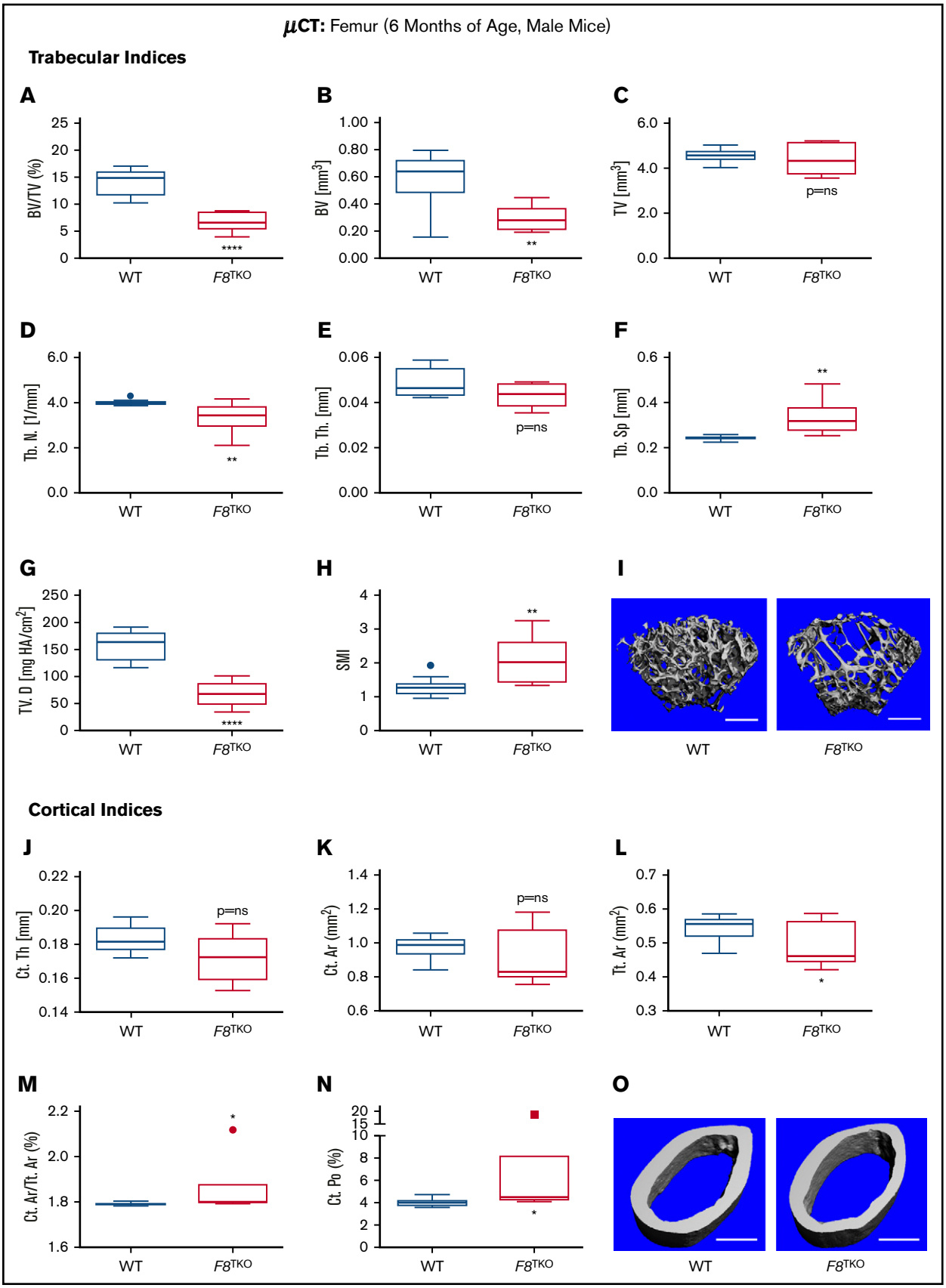

Figure 2.

Cortical bone was quantified at the femoral middiaphysis from 99 tomographic slices (total area of 0.6 mm).

Biochemical indices of bone turnover and sex steroid quantifications

C-terminal telopeptide of collagen type I (CTX; a bone resorption marker) and serum N-terminal propeptide of type 1 procollagen (PINP; a bone formation marker) were quantified using enzyme immunoassays from Immunodiagnostic Systems (Gaithersburg, MD). 17β-estradiol was quantified in female mice serum using an enzyme-linked immunosorbent assay (ab108667) from Abcam (Cambridge, MA) and testosterone in male mice serum using an enzyme-linked immunosorbent assay (11-TESHU-E01) from ALPCO (Salem, NH).

Statistical analysis

Statistical analysis was performed using Prizm-V7 (GraphPad Software, La Jolla, CA). Simple comparisons between WT and $F8^{TKO}$ mice involved an unpaired, 2-tailed Student *t* test for parametric data. Data distributions were assessed using a Shapiro-Wilk normality test and nonparametric data assessed using a Mann-Whitney *U* test (as indicated). $P \leq .05$ was considered statistically significant. No outliers are removed, and all data points are included in graphics and statistical analyses unless indicated. Data are presented as boxplots (median + interquartile range [IQR]) with Tukey whiskers and outliers presented as individual data points per convention.

Results

Skeletally mature $F8^{TKO}$ male mice have significantly diminished vertebral cortical and trabecular bone mass and diminished trabecular bone mass in the femur

To study the etiology, kinetics, and mechanisms of bone loss in HA, we used the $F8^{TKO}$ mouse model of FVIII deficiency and performed high-resolution (6-μm) μCT analysis of the L3 vertebrae and distal femoral metaphasis and middiathesis in skeletally mature (6-month-old) male $F8^{TKO}$ and WT control mice.

Our data show that the trabecular bone volume (BV) fraction (BV/TV), a key index of trabecular bone mass, was significantly diminished in the L3 vertebrae of male $F8^{TKO}$ mice (Figure 1A). Diminished bone mass was accounted for by a significant decline in trabecular BV (Figure 1B) rather than a change in the size of the trabecular compartment (total BV [TV]) (Figure 1C). Analysis of trabecular bone microarchitecture revealed a decline in trabecular number (Tb.N) (Figure 1D) and trabecular thickness (Tb.Th) (Figure 1E) with a corresponding increase in trabecular separation (Tb.Sp) (Figure 1F). Trabecular volumetric bone density (TV.D) was also significantly diminished (Figure 1G), and the structure model index (SMI), a reflection of the geometrical rod/plate-like nature of the trabecular structure, was significantly increased, reflecting an inherently weaker geometrical conformation. Representative 3D reconstructions of the vertebral trabecular compartment are shown in Figure 1I.

Trabecular analysis of the distal femoral metaphases revealed data essentially identical to that in the vertebrae (Figure 2A-I), suggesting a significant deficit of trabecular bone in both the axial and appendicular skeletons.

Further analysis of the cortical bone compartment in the L3 vertebrae also reveal diminished cortical bone structure in $F8^{TKO}$ mice. Specifically, average cortical thickness (Ct.Th) (but not cortical area [Ct.Ar]) and the total cross-sectional area inside the periosteal envelope (Tt.Ar) were all significantly diminished (Figures 1J-L). Although both Ct.Ar and Tt.Ar were significantly decreased, the Ct.Ar fraction (Ct.Ar/Tt.Ar) was significantly increased, suggesting a more pronounced decline in Tt.Ar than in Ct.Ar (Figure 1M). Cortical porosity was also significantly increased (Figure 1N), reflecting denuded structure.

In the axial skeleton, trabecular bone and vertebrae were similarly diminished (Figure 2A-I); however, the cortical compartment of the femoral diathesis was less markedly affected, with only Tt.Ar (Figure 2L) showing a significant decline and Ct.Ar/Tt.Ar and Ct.Po (Figure 2M-N) showing a significant increase.

Taken together, our data reveal that at 6 months of age (a time when WT C57BL6 mice have reached peak BMD and optimal mechanical properties[22]), male $F8^{TKO}$ mice have a dramatic deficit in trabecular bone in both vertebrae and femur. Furthermore, vertebrae also suffered from a significant deficit in cortical bone mass, although the femurs were less severely impacted.

Female $F8^{TKO}$ mice have diminished cortical bone in their femurs and vertebrae

Little is known regarding bone health in severe female HA patients. We thus examined bone structure in female $F8^{TKO}$ mice using μCT. In contrast to male mice, female $F8^{TKO}$ mice at 6 months of age had no significant alterations in BV/TV or BV in the vertebrae (Figure 3A-B), although a small but significant decline in TV (Figure 3C) was noted, suggesting a smaller trabecular compartment, but with relatively normal BV within that compartment. Tb.Th and Tb.Sp were both significantly diminished, although Tb.Sp typically moves in the opposite direction and may be related to the diminished TV. SMI was also significantly increased (Figure 3H), suggesting a conversion of plates to a weaker rod-like geometry. By contrast, the vertebral cortical compartment was robustly impacted, with Ct.Th, Ct.Ar, and Tt.Ar all significantly diminished (Figure 3J-L) and Ct.Ar/Tt.Ar and Ct.Po (Figure 3M-N) significantly increased.

Similar data were seen in the femur, with a significant decline in TV (Figure 4C). As in the vertebrae, the cortical compartment of the femur was more robustly diminished (but less so than the

Figure 2. μCT analysis of femur in skeletally mature WT and $F8^{TKO}$ male mice. Six-month-old male C57BL6 WT and $F8^{TKO}$ mice femurs were analyzed by high-resolution (6-μm) μCT for trabecular bone in the distal metaphysis and cortical bone at middiaphysis. (A-H) Trabecular indices (A) BV/TV, (B) BV, (C) TV, (D) Tb.N, (E) Tb.Th, (F) Tb.Sp, (G) TV.D, and (H) SMI. (I) Representative high-resolution (6-μm) 3D visual reconstructions of trabecular bone. Scale bars represent 500 μm. (J-N) Cortical indices (J) Ct.Th, (K) Ct.Ar, (L) Tt.Ar, (M) Ct.Ar/Tt.Ar, and (N) Ct.Po. (O) Representative high-resolution (6-μm) 3D visual reconstructions of cortical bone. Scale bars represent 500 μm. Data are expressed as boxplots (median + IQR) with Tukey whiskers. n = 10 WT and 6 $F8^{TKO}$ mice/group. $^*P < .05$, $^{**}P < .01$, $^{****}P < .0001$, and ns by Student *t* test or Mann-Whitney *U* test (Ct.Ar/Tt.Ar and Ct.Po).

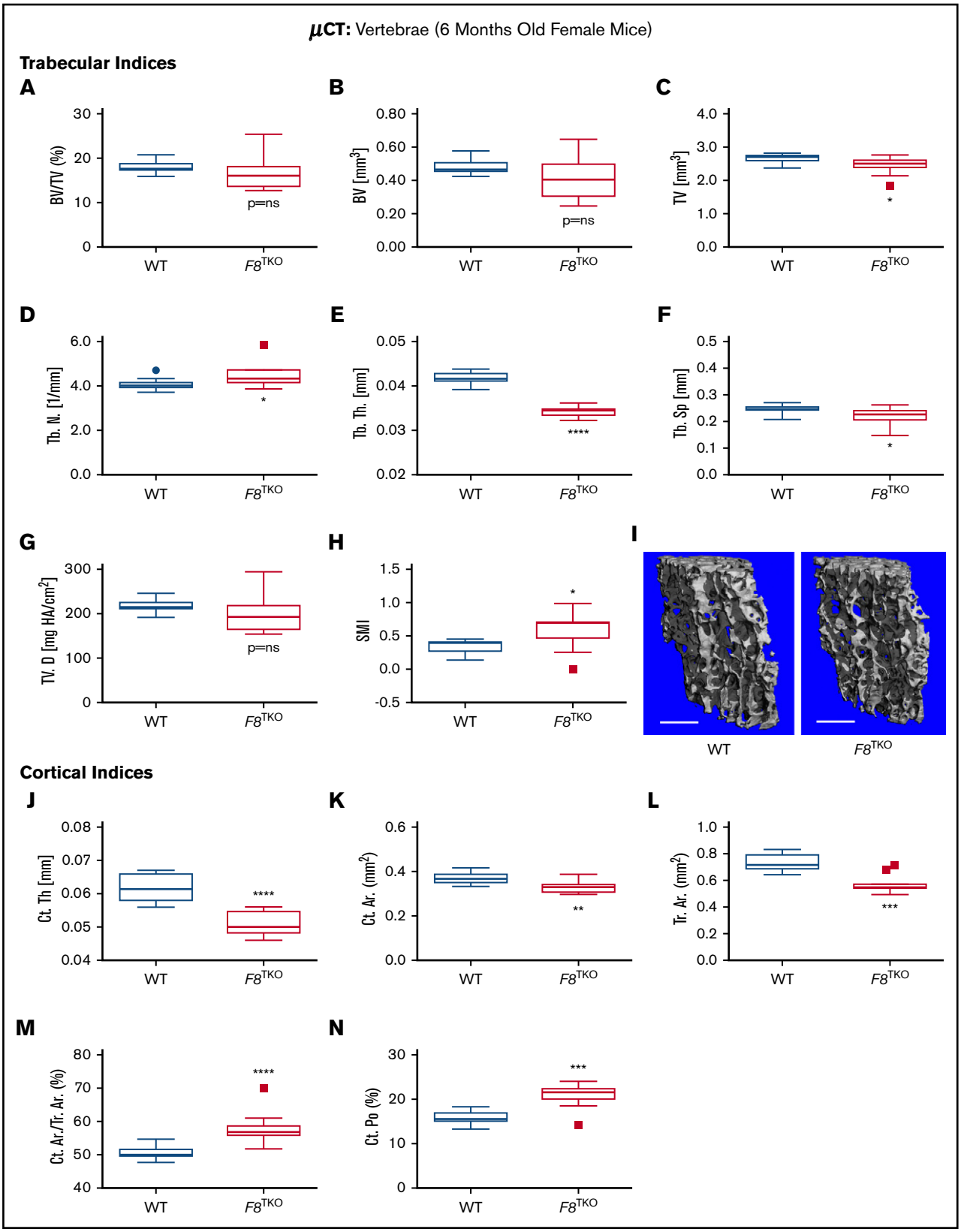

Figure 3. μCT analysis of lumbar vertebrae in skeletally mature WT and *F8*^{TKO} female mice. Six-month-old female C57BL6 WT and *F8*^{TKO} mice L3 vertebrae were analyzed by high-resolution (6-μm) μCT and independent trabecular and cortical bone compartments segregated. (A-H) Trabecular indices (A) BV/TV, (B) BV, (C) TV, (D) Tb.N, (E) Tb.Th, (F) Tb.Sp, (G) TV.D, and (H) SMI. (I) Representative high-resolution (6-μm) 3D visual reconstructions of L3 vertebrae. Scale bars represent 500 μm.

vertebrae), with significant declines in Ct.Ar and in Tt.Ar being evident (Figure 4K-L).

Taken together, our data reveal a sexual dimorphic effect of *F8* depletion, with female mice experiencing a preferential loss of cortical bone and males undergoing both cortical and trabecular bone loss. In both sexes, cortical bone in the vertebrae was more aggressively impacted than in the femurs.

Young (2-month-old) *F8*^{TKO} male and female mice do not show significant deficits in BV

To determine whether the bone loss observed in mature *F8*^{TKO} mice was associated with defects in early bone patterning or early bone modeling, we analyzed trabecular and cortical bone in femurs from young (2-month-old) male and female WT and *F8*^{TKO} mice by μCT. In male mice, no changes in BV/TV or BV were noted (supplemental Figure 1A-B); however, TV, a reflection of the size of the trabecular compartment, was already significantly diminished (supplemental Figure 1C). Consistent with unaltered BV and BV/TV, the structural indices Tb.N, Tb.Th, and Tb. Sp, as well as TV.D and SMI, were all unchanged (supplemental Figure 1D-H). In addition, no indices of cortical bone structure were altered at this age (supplemental Figure 1J-O).

Similar to male mice, at 2 months of age, no trabecular or cortical indices were altered in the femur of female mice (supplemental Figure 2).

Taken together, the data suggest that alterations in bone mass in male and female *F8*^{TKO} mice develop during the late bone modeling period and cause a failure to attain peak bone mass, which typically occurs at ~4 to 5 months of age in mice.[22]

BMD quantified by DXA is not significantly altered in male *F8*^{TKO} mice but was significantly affected in female mice

As DXA technology is commonly used in humans to assess bone condition, we also performed ex vivo DXA analysis of the lumbar spine, femurs, and tibias from male and female WT and *F8*^{TKO} mice. Although there was a strong trend toward significance ($P = .0763$) in the lumbar spine of male mice, none of the anatomical sites (lumbar spine, femur, or tibia; Figure 5A-C) were significantly different from WT in 6-month-old mice.

By contrast, female mice had significantly diminished bone loss at all sites (lumbar spine, femur, and tibia; Figures 5D-F).

Bone formation markers are suppressed in male *F8*^{TKO} mice, but bone resorption markers are increased in female *F8*^{TKO} mice, with sex steroids diminished in both

To assess whether the deficit in BV is a consequence of a decline in bone formation, an increase in bone resorption, or a combination of both, we quantified metabolic bone turnover indices of bone formation (PINP) and resorption (CTX) in the serum of 2- and 6-month-old male and female WT and *F8*^{TKO} mice. Although no significant defects in trabecular or cortical BV were observed at 2 months of age in male mice, the bone formation marker (PINP) was already found to be significantly diminished ($\Delta = -6.3\%$) (Figure 6A). By 6 months of age, the magnitude of the change in PINP had further decreased ($\Delta = -20.3\%$) relative to WT levels (Figure 6C).

By contrast, CTX was unchanged at both 2 months (Figure 6B) and 6 months of age (Figure 6D). These data suggest that the declines in bone mass in male *F8*^{TKO} mice are a consequence of a decrease in bone formation rather than effects on bone resorption.

By contrast, PINP was not significantly different from WT mice in female *F8*^{TKO} mice at either 2 or 6 months of age (Figure 6E,G). However, there was a strong trend toward increased bone resorption (CTX) at 2 months, which attained statistical significance by 6 months (Figure 6F,H).

As sex hormones play key roles in regulation of the skeleton, we quantified 17β-estradiol in female and testosterone in male WT and *F8*^{TKO} mice serum at 2 and 6 months of age. Neither 17β-estradiol nor testosterone was significantly different between groups at 2 months of age (Figure 6I,K), although there was considerable variability in testosterone in the WT group. However, by 6 months, *F8*^{TKO} mice had significantly lower 17β-estradiol (Figure 6J) and testosterone (Figure 6L) concentrations, suggesting that sex steroid decline may contribute to bone loss in both male and female *F8*^{TKO} mice.

Quantitative bone histomorphometry confirms significant suppression of bone formation in male *F8*^{TKO} mice

PINP is a global marker of bone formation across all bone surfaces in the body. To confirm a decline in bone formation in male mice in a more rigorous manner, we used quantitative bone histomorphometry, the gold standard for assessment of bone formation at the tissue level. Histomorphometry is a 2-dimensional technique and lacks the 3-dimensional volumetric capabilities of μCT for evaluation of structural indices. Nonetheless, femurs from 6-month-old WT and *F8*^{TKO} mice had significantly diminished bone area and BV/TV (but not tissue area), confirming diminished trabecular BV in *F8*^{TKO} mice (Figure 7A-C). Importantly, the 2 key dynamic indices of bone formation, MAR and BFR normalized for BS, were significantly diminished in *F8*^{TKO} mice (Figure 7D-E). Representative photomicrographic images of calcein-labeled bones from WT and *F8*^{TKO} mice, from which MAR and BFR/BS were calculated, are shown in Figure 7F.

Interestingly, the static indices osteoblast number and osteoblast surface, both normalized for BS, were not significantly different from WT mice (Figure 7G-H), suggesting that the activity of the osteoblasts is suppressed rather than a decline their differentiation.

Two static indices of osteoclasts, osteoclast number and osteoclast surface, both normalized for BS (Figure 7I-J), did not reveal any

Figure 3. (continued) (J-N) Cortical indices (J) Ct.Th, (K) Ct.Ar, (L) Tt.Ar, (M) Ct.Ar fraction (Ct.Ar/Tt.Ar), and (N) cortical porosity (Ct.Po). All data are expressed as boxplots (median + IQR) with Tukey whiskers. n = 10 WT and 11 *F8*^{TKO} mice/group. *$P < .05$, **$P < .01$, ***$P < .001$, ****$P < .0001$, and ns by Student *t* test or Mann-Whitney *U* test (Tb.N, Tt.Ar, and Ct.Ar/Tt.Ar).

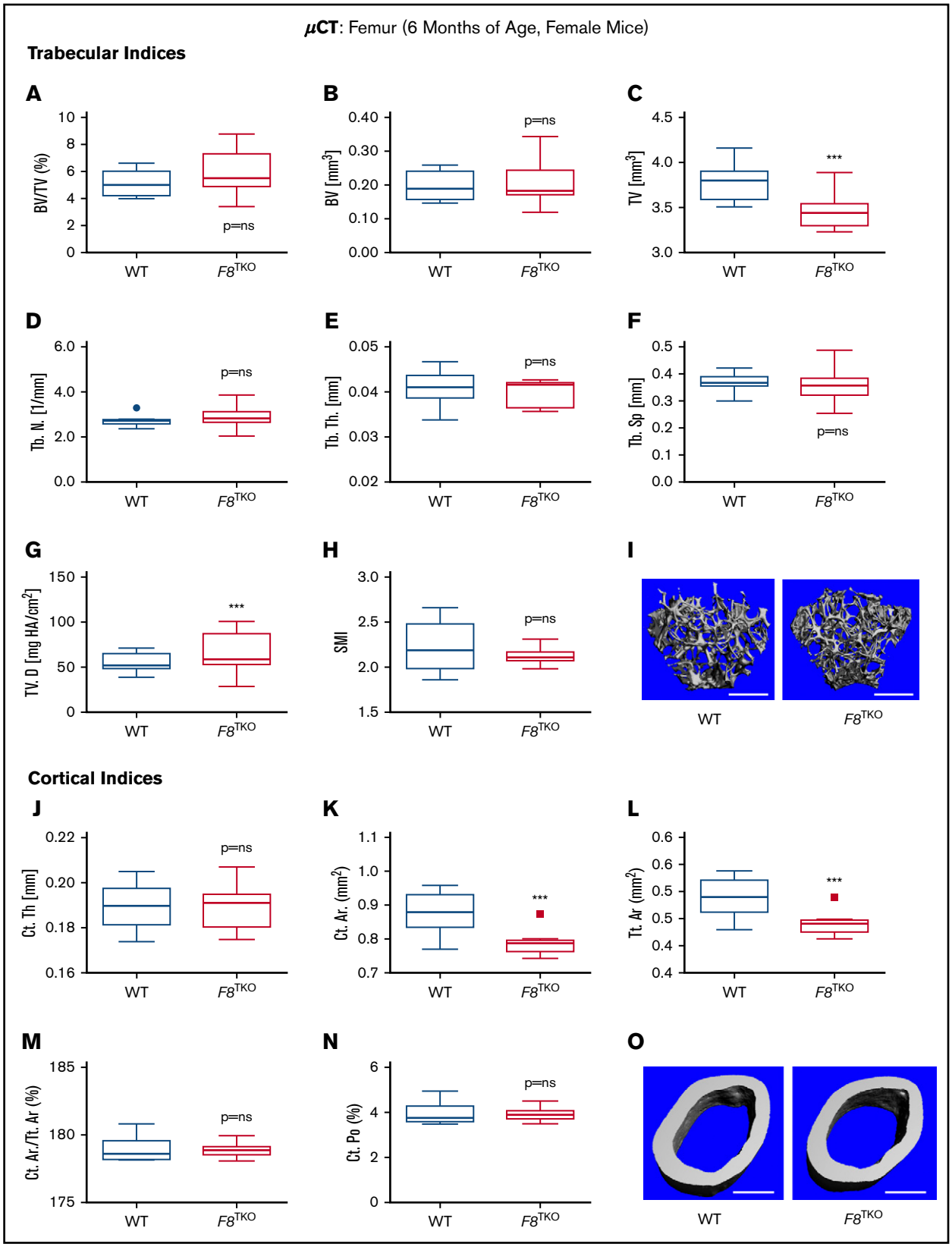

Figure 4. μCT analysis of femur in skeletally mature WT and *F8*^{TKO} female mice. Six-month-old female C57BL6 WT and *F8*^{TKO} mice femurs were analyzed by high-resolution (6-μm) μCT for trabecular bone in the distal metaphysis and cortical bone at middiaphysis. (A-H) Trabecular indices (A) BV/TV, (B) BV, (C) TV, (D) Tb.N, (E) Tb.Th, (F) Tb.Sp, (G) TV.D, and (H) SMI. (I) Representative high-resolution (6-μm) 3D visual reconstructions of trabecular bone. Scale bars represent 500 μm.

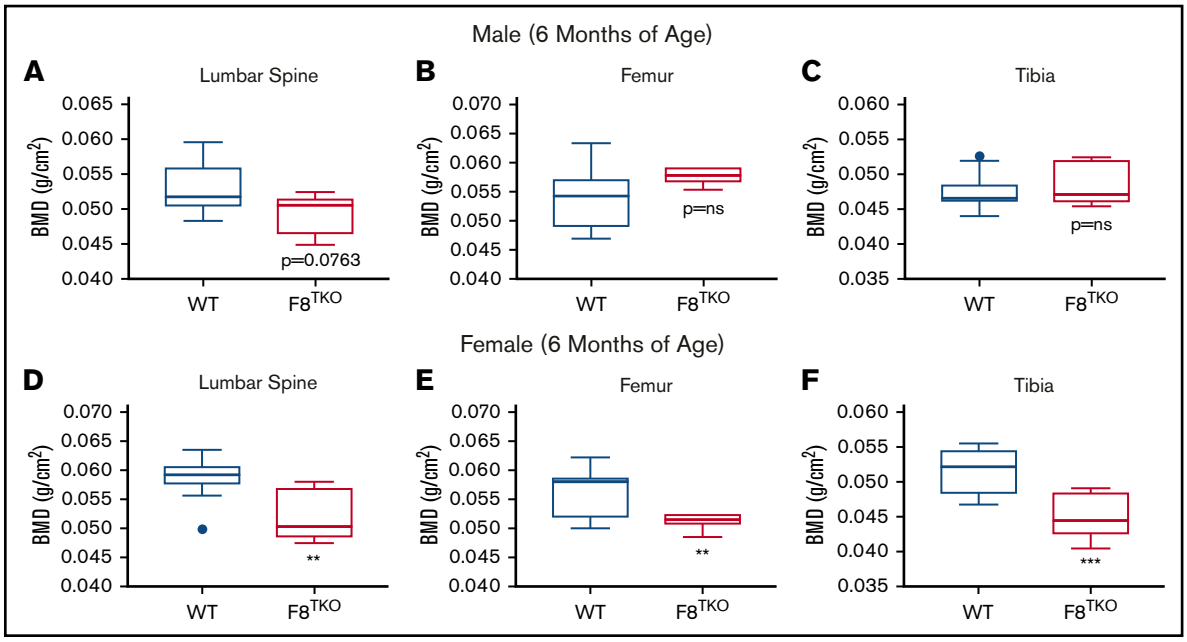

Figure 5. BMD quantified by DXA in lumbar spine, femurs, and tibias of skeletally mature male and female WT and *F8*^{TKO} male mice. (A-F) BMD was assessed ex vivo by DXA in 6-month-old male C57BL6 WT and *F8*^{TKO} mice in lumbar spine (A), femur (B), and tibia (C) and in 6-month-old female mice in lumbar spine (D), femur (E), and tibia (F). Data are expressed as boxplots (median + IQR) with Tukey whiskers. n = 10 male and female WT and 5 male and 7 female *F8*^{TKO} mice/group. ns by Student *t* test or Mann-Whitney *U* test (male tibia).

significant changes, although high sample variability was observed in *F8*^{TKO} mice, and a trend toward increased osteoclast number and osteoclast surface was evident.

Taken together, our histomorphometry data support a model in which a decline in bone formation in male *F8*^{TKO} mice, leads to a significant loss of BV and mass, preventing the attainment of peak bone mass in the mature skeletons of male *F8*^{TKO} mice. By contrast, the data suggest that in female mice, an increase in bone resorption rather than a decline in bone formation, is responsible for the resulting bone loss.

Discussion

Low BMD and an increased incidence of fractures are common in patients with HA.[6,23] However, the mechanisms and etiology are not well understood. In this study, we made use of a mouse model of severe HA to study the effects of complete FVIII deficiency on bone mass and turnover in male and female mice in the absence of multiple confounders for low BMD that are common in human HA populations. The data confirm that deficiency of FVIII leads to altered bone metabolism. Furthermore, our data reveal that a progressive decline in bone formation, beginning in the postnatal bone modeling period and increasing in magnitude with time, is the primary defect that leads to a deficit in skeletal bone mass in male mice. By contrast, we found no significant changes in bone resorption. While both trabecular and cortical bone mass was robustly diminished in the vertebrae of male *F8*^{TKO} mice, femurs developed a significant deficit in trabecular bone mass, with a relatively milder bone loss observed in cortical bone.

By contrast, an increase in bone resorption was the primary defect causing bone loss in female mice, and interestingly, cortical bone was more significantly impacted than trabecular bone in both femur and vertebrae. These differences in cortical and trabecular bone are likely related to the different mechanisms of bone loss between males (reduced formation) and females (increased resorption). Although the mechanism remains to be characterized in detail, significant declines in sex steroids (17β-estradiol and testosterone in female and male mice, respectively) may underlie, or contribute to, the increased bone resorption in female mice and diminished bone formation in males. If validated in humans, sex steroid replacement may be a viable therapeutic approach to alleviating bone loss in both men and women with HA.

Irrespective of the sexual dimorphism in mechanism, both male and female mice failed to attain peak BMD due to their respective disruptions in bone turnover during bone modeling. Failure to attain peak BMD is a significant risk factor for fracture later in life, and ensuring that peak BMD is achieved may be critical to the future skeletal health of HA patients.[5]

Our data in male mice conflict, in part, with previous histomorphometric and bone turnover studies in another animal model of HA.[19,20] In a previous study, it was concluded that bone loss in HA

Figure 4. (continued) (J-N) Cortical indices (J) Ct.Th, (K) Ct.Ar, (L) Tt.Ar, (M) Ct.Ar/Tt.Ar, and (N) Ct.Po. (O) Representative high-resolution (6-μm) 3D visual reconstructions of cortical bone. Scale bars represent 500 μm. Data are expressed as boxplots (median + IQR) with Tukey whiskers. n = 10 WT and 11 *F8*^{TKO} mice/group. ***$P < .001$ and ns by Student *t* test or Mann-Whitney *U* test (Tb.Th, Ct.Ar, Tt.Ar, Ct.Ar/Tt.Ar, and Ct.Po).

Figure 6. Biochemical bone turnover markers and sex steroid concentrations in skeletally mature WT and *F8*^{TKO} male mice. Biochemical indices of bone turnover (resorption and formation) were quantified in serum from 2-month-old and 6-month-old male and female C57BL6 WT and *F8*^{TKO} mice. The bone formation marker PINP in males at 2 months (A) and 6 months (C). The bone resorption marker CTX in males at 2 months (B) and 6 months (D). PINP in females at 2 months (E) and 6 months (G). CTX in females at 2 months (F) and 6 months (H). Data are expressed as boxplots (median + IQR) with Tukey whiskers. n = 10 WT and 6 *F8*^{TKO} male mice/group and 10 WT and 11 *F8*^{TKO} female mice at 6 months, and 10 WT and 12 *F8*^{TKO} male mice/group and 10 WT and 6 at *F8*^{TKO} female mice at 2 months. **P* < .05 by Student *t* test. Quantitative analysis of 17β-estradiol and testosterone concentrations in serum from young and mature WT and *F8*^{TKO} male mice. (I-J) To quantify sex steroid concentrations, we measured 17β-estradiol in serum from female WT and F8^{TKO} mice at 2 months of age (I) and 6 months of age (J). (K-L) Testosterone was quantified in male mouse serum at 2 months of age (K) and 6 months of age (L). Data are expressed as boxplots (median + IQR) with Tukey whiskers. n = 10 WT and 6 F8^{TKO} male mice/group and 20 WT and 8 F8^{TKO} female mice at 2 months, and 10 WT and 6 F8^{TKO} male mice/group and 20 WT and 10 at F8^{TKO} female mice at 6 months. **P* < .05, ***P* < .01, and ns by Student *t* test (female mice) or Mann-Whitney *U* test (male mice). One extreme (6-month-old male F8^{TKO} group outlier [11.6 ng/mL: Grubbs test, α = 0.05]) was removed from the statistical analysis but is shown on the graph.

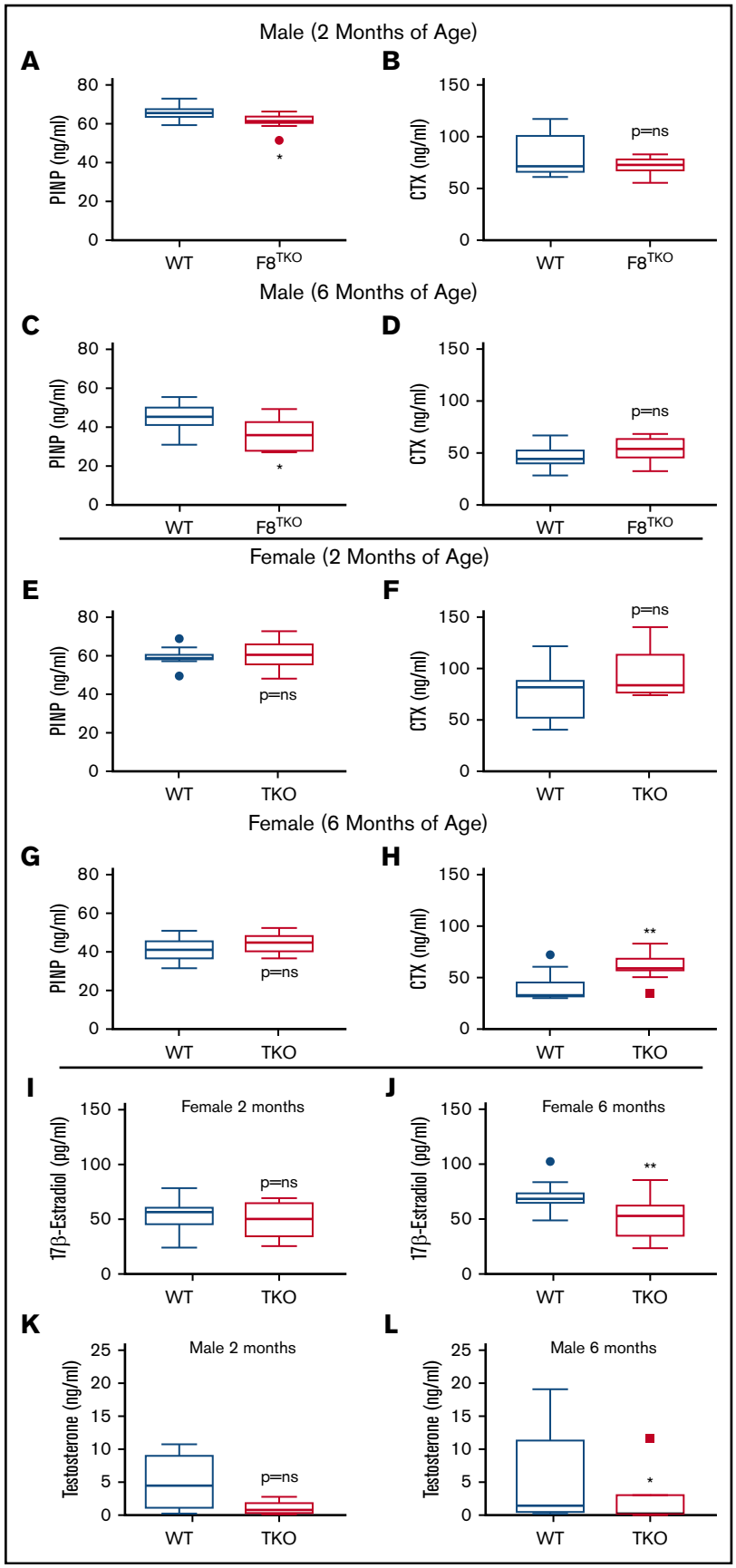

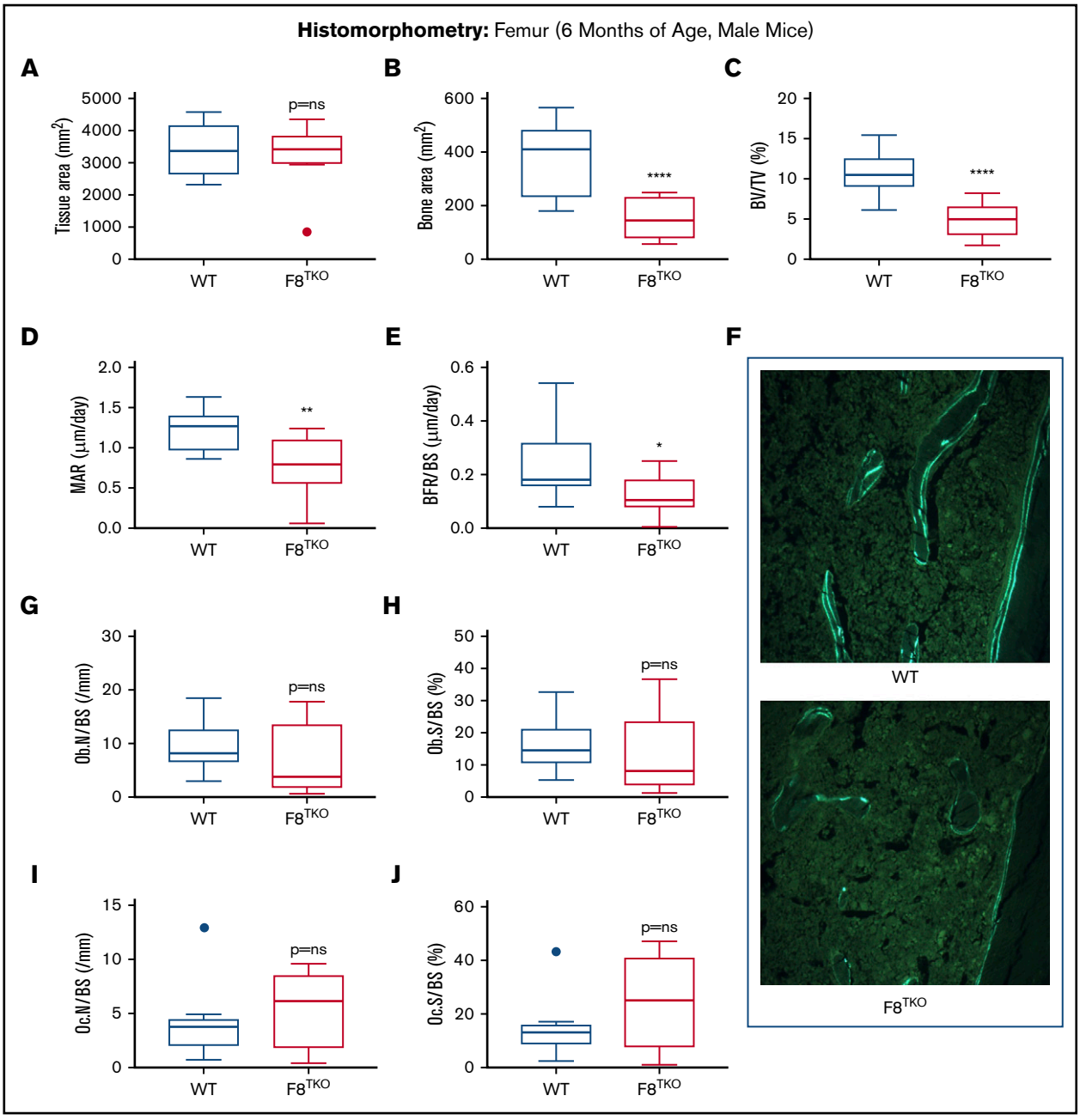

Figure 7. Quantitative bone histomorphometry of skeletally mature WT and *F8*^{TKO} male mice. Histomorphometric indices of bone formation and resorption were quantified in femurs of 6-month-old male WT and *F8*^{TKO} mice. Dynamic osteoblast measurements were made in calcein-labeled unstained plastic-embedded sections and static indices in sections stained with VonKossa/MacNeals Tetrachrome. The following osteoclast indices were quantified in deplasticized sections stained for tartrate-resistant acid phosphatase and counterstained with fast green: (A) tissue area, (B) bone area, (C) BV/TV, (D) MAR, (E) BFR/BS, (F) representative images of double calcein-labeled bone sections. Magnification: 20× objective (original magnification ×200 final), (G) osteoblast number (N.Ob), (H) osteoblast surface (Ob.S), (I) osteoclast number (Oc.N)/BS, and (J) osteoclast surface (Oc.S)/BS. Data are expressed as boxplots (median + IQR) with Tukey whiskers. n = 10 WT and 10 *F8*^{TKO} mice/group. *$P < .05$, **$P < .01$, and ****$P < .0001$ by Student *t* test.

was secondary to increased bone resorption in male mice, as changes in bone formation indices were not statistically significant.[20] There are several possible reasons why our data may differ from the previous mouse study. Firstly, different mouse models alone may account for these discrepancies. The previous study used animals with a truncated or partially deleted *F8*, whereas ours used animals in which there was a complete deletion. The partial synthesis of defective FVIII proteins, irrespective of functionality, may have promoted an inflammatory state driving up resorption, whereas in our model, no FVIII protein is generated at all, potentially amplifying the formation defect. As genetics play a critical role in bone mass and turnover, strain differences could also contribute to

the different outcomes; Recht et al used a mouse on a mixed C57BL/6/S129 background,[20] while our model was backcrossed to near homogeneity on the C57BL6 background and used carefully matched WT littermate controls. Additional variables, such as esoteric as microbiota differences between animal vendors and institutional housing facilities, are now recognized to have significant effects on bone turnover and mass in mice.[24]

Our animal data are consistent with at least one clinical study reporting that low levels of the bone formation marker osteocalcin predominated in children with low BMD, while no differences were identified with regard to the bone resorption marker CTX. Furthermore, the bone formation marker, but not the bone resorption marker, was found to account for 10% of the variation in lumbar spine Z-scores in this population.[15]

In another study of BMD and bone turnover in HA patients, reduced markers of bone formation (osteocalcin) were also identified, but there was also evidence of increased markers of bone resorption.[14] However, a significant caveat of this study was that 40% of the HA patients were also infected with HIV,[14] an established cause of a dramatic increase in bone resorption,[11,13] and HIV infection could hence account for much of the increased resorption observed in this HA study.

Given the key role played by genetics in regulating skeletal mass and turnover, total F8 deficiency may likely produce a different phenotype than that of partial F8 deficiency, as appears to occur in mice models. However, in humans, confounders for low BMD associated with lifestyle factors, hemophilia-related interventions, racial and ethnic differences, different microbiota, different grades of hemophilia severity, and others may compound or dominate the genetic effects.

The mechanism of bone loss in HA is thus important, because the mode of therapy may need to be tailored to the mechanism driving bone loss. For example, patients with predominantly bone formation defects may benefit from bone anabolic drugs that promote bone formation such as teriparatide. By contrast, patients with primarily osteoclastic resorption phenotypes may respond better to anticatabolic drugs such as bisphosphonates or denosumab, which prevent excessive bone resorption. Although, antiresorptive agents such as the bisphosphonate ibandronate have been used successfully to treat bone loss in HA patients, the use of bone anabolic drugs to offset low bone formation may need to be considered in some patients with low bone formation who fail to achieve peak BMD.

Although μCT is a high-resolution technology that can provide detailed microarchitectural and structural data, clinical definitions of osteopenia and osteoporosis are derived from DXA-based BMD T-scores (or Z-scores in children). Because the highly metabolically active trabecular compartment makes up only 20% of bone mass, it is underestimated by DXA, which may explain why we were unable to detect changes in BMD by DXA in male mice but were able to detect effects on trabecular bone by μCT. By contrast, owing to the predominance of cortical bone decline in female mice, DXA was capable of detecting changes. As changes in trabecular bone may act as a sentinel for early bone disease, clinical assessments using DXA may underestimate skeletal damage in humans, especially in the trabecular compartment, leading to delayed interventions.

In conclusion, our data demonstrate that both male and female $F8^{TKO}$ mice fail to achieve peak bone mass and optimal load-bearing structure at key anatomic sites susceptible to fracture in humans, including the femur and spine. The mechanisms involved, however, are different, with diminished bone formation in the case of males and increased bone resorption in females. Assessment of bone turnover in osteoporotic human HA patients may be important to establish the appropriate therapeutic strategy to stop bone loss and to promote attainment of peak BMD in children with HA.

Acknowledgments

The authors thank Penny Roon and the Augusta University Electron Microscopy and Histology Core Laboratory for preparation of histological sections for histomorphometry.

M.N.W. was supported in part by the Biomedical Laboratory Research & Development Service of the VA Office of Research and Development (grant 5I01BX000105) and by the National Institute of Arthritis and Musculoskeletal and Skin Diseases, National Institutes of Health (grants AR068157 and AR070091). M.E.M.-L. was supported by the National Institute on Aging, National Institutes of Health (grant AG036675).

The content of this publication does not represent the views of the Department of Veterans Affairs, the National Institutes of Health, or the US Government.

Authorship

Contribution: M.N.W. and C.L.K. conceived the study; M.N.W. performed data analysis and drafted the manuscript; C.L.K. and D.W. edited the manuscript; S.R.-P., T.V., D.W., L.H., W.H.B., N.d.M.A., K.Y., and M.E.M.-L. performed data acquisition; S.L.M. provided unique reagents; and all authors read, revised, and approved the manuscript.

Conflict-of-interest disclosure: S.L.M. has performed consulting for Bayer, Shire, Grifols, HEMA Biologics, Bioverativ, CSL Behring, Novo Nordisk, and Genentech. The remaining authors declare no competing financial interests.

ORCID profile: M.N.W., 0000-0003-3305-5748.

Correspondence: M. Neale Weitzmann, Department of Medicine, Emory University School of Medicine, 1305 WMRB, 101 Woodruff Cir, Atlanta, GA 30322; e-mail: mweitzm@emory.edu.

References

1. Chao BN, Baldwin WH, Healey JF, et al. Characterization of a genetically engineered mouse model of hemophilia A with complete deletion of the F8 gene. *J Thromb Haemost*. 2016;14(2):346-355.

2. Hoyer LW. Hemophilia A. *N Engl J Med*. 1994;330(1):38-47.

3. Di Michele DM, Gibb C, Lefkowitz JM, Ni Q, Gerber LM, Ganguly A. Severe and moderate haemophilia A and B in US females. *Haemophilia*. 2014;20(2):e136-e143.

4. Soucie JM, Nuss R, Evatt B, et al; The Hemophilia Surveillance System Project Investigators. Mortality among males with hemophilia: relations with source of medical care. *Blood*. 2000;96(2):437-442.

5. Raisz LG. Pathogenesis of osteoporosis: concepts, conflicts, and prospects. *J Clin Invest*. 2005;115(12):3318-3325.

6. Kempton CL, Antun A, Antoniucci DM, et al. Bone density in haemophilia: a single institutional cross-sectional study. *Haemophilia*. 2014;20(1):121-128.

7. Gerstner G, Damiano ML, Tom A, et al. Prevalence and risk factors associated with decreased bone mineral density in patients with haemophilia. *Haemophilia*. 2009;15(2):559-565.

8. Caviglia H, Landro ME, Galatro G, Candela M, Neme D. Epidemiology of fractures in patients with haemophilia. *Injury*. 2015;46(10):1885-1890.

9. Bass E, French DD, Bradham DD, Rubenstein LZ. Risk-adjusted mortality rates of elderly veterans with hip fractures. *Ann Epidemiol*. 2007;17(7): 514-519.

10. Dempster DW. Osteoporosis and the burden of osteoporosis-related fractures. *Am J Manag Care*. 2011;17(Suppl 6):S164-S169.

11. Ofotokun I, Titanji K, Vikulina T, et al. Role of T-cell reconstitution in HIV-1 antiretroviral therapy-induced bone loss. *Nat Commun*. 2015;6(1):8282.

12. Ofotokun I, Titanji K, Vunnava A, et al. Antiretroviral therapy induces a rapid increase in bone resorption that is positively associated with the magnitude of immune reconstitution in HIV infection. *AIDS*. 2016;30(3):405-414.

13. Weitzmann MN, Ofotokun I. Physiological and pathophysiological bone turnover - role of the immune system. *Nat Rev Endocrinol*. 2016;12(9):518-532.

14. Katsarou O, Terpos E, Chatzismalis P, et al. Increased bone resorption is implicated in the pathogenesis of bone loss in hemophiliacs: correlations with hemophilic arthropathy and HIV infection. *Ann Hematol*. 2010;89(1):67-74.

15. Tlacuilo-Parra A, Villela-Rodríguez J, Garibaldi-Covarrubias R, Soto-Padilla J, Orozco-Alcala J. Bone turnover markers and bone mineral density in children with haemophilia. *Haemophilia*. 2011;17(4):657-661.

16. Alioglu B, Selver B, Ozsoy H, Koca G, Ozdemir M, Dallar Y. Evaluation of bone mineral density in Turkish children with severe haemophilia A: Ankara hospital experience. *Haemophilia*. 2012;18(1):69-74.

17. Avgeri M, Papadopoulou A, Platokouki H, et al. Assessment of bone mineral density and markers of bone turnover in children under long-term oral anticoagulant therapy. *J Pediatr Hematol Oncol*. 2008;30(8):592-597.

18. Christoforidis A, Economou M, Papadopoulou E, et al. Comparative study of dual energy X-ray absorptiometry and quantitative ultrasonography with the use of biochemical markers of bone turnover in boys with haemophilia. *Haemophilia*. 2011;17(1):e217-e222.

19. Liel MS, Greenberg DL, Recht M, Vanek C, Klein RF, Taylor JA. Decreased bone density and bone strength in a mouse model of severe factor VIII deficiency. *Br J Haematol*. 2012;158(1):140-143.

20. Recht M, Liel MS, Turner RT, Klein RF, Taylor JA. The bone disease associated with factor VIII deficiency in mice is secondary to increased bone resorption. *Haemophilia*. 2013;19(6):908-912.

21. Roser-Page S, Vikulina T, Zayzafoon M, Weitzmann MN. CTLA-4Ig-induced T cell anergy promotes Wnt-10b production and bone formation in a mouse model. *Arthritis Rheumatol*. 2014;66(4):990-999.

22. Brodt MD, Ellis CB, Silva MJ. Growing C57Bl/6 mice increase whole bone mechanical properties by increasing geometric and material properties. *J Bone Miner Res*. 1999;14(12):2159-2166.

23. Gay ND, Lee SC, Liel MS, Sochacki P, Recht M, Taylor JA. Increased fracture rates in people with haemophilia: a 10-year single institution retrospective analysis. *Br J Haematol*. 2015;170(4):584-586.

24. Sjögren K, Engdahl C, Henning P, et al. The gut microbiota regulates bone mass in mice. *J Bone Miner Res*. 2012;27(6):1357-1367.